A Stochastic Multi-Commodity Logistic Model for Disaster Preparation in Distribution Systems

Anmar Arif, *Student Member, IEEE*, Zhaoyu Wang, *Member, IEEE*, Chen Chen, *Member, IEEE*, and Bo Chen, *Member, IEEE*

***Abstract*—This paper proposes a stochastic optimization approach for disaster preparation in distribution systems. For an upcoming storm, utilities should have a preparation plan that includes warehousing restoration supplies, securing staging sites (depots), and prepositioning crews and equipment. Pre-storm planning enables faster and more efficient post-disaster deployment of crews and equipment resources to damage locations. To assist utilities in making this important preparation, this paper develops a two-stage stochastic mixed integer linear program. The first stage determines the depots, number of crews in each site, and the amount of equipment. The second stage is the recourse action that deals with acquiring new equipment and assigning crews to repair damages in realized scenarios. The objective of the developed model is to minimize the costs of depots, crews, equipment, and penalty costs associated with delays in obtaining equipment and restoration. We consider the uncertainties of damaged lines, number and type of equipment required, and expected repair times. The model is validated on modified IEEE 123-bus distribution test system.**

***Index Terms*—Allocation, disaster preparation, distribution system, extreme weather, stochastic programming.**

Nomenclature

Indices and Sets

k, c, s, τ	Indices for distribution line, crew, scenario and resource type
d/e	Indices for depot (staging site)
C^L, C^T, IC	Set of line crews, tree crews, and internal crews
Ω_{CD}, Ω_P	Set of buses with critical loads and set of depots
$\Omega_L^c(k), \Omega_L^p(k)$	Set of conductors and poles in line k.

Parameters

$\mathcal{C}_d^E, \mathcal{C}_d^H$	The capacity of depot d for storing the supplies and capacity for accommodating the crews
$\mathcal{C}_\tau^R$	The capacity required to store resource τ
$D_{k,n}$	Distance between components k and n damaged line
$\bar{D}$	Maximum distance allowed between a crew's location and assigned damaged line
$ET_{k,s}^L, ET_{k,s}^T$	Estimated time to repair line k for line and tree crews
$E_{d,\tau}^0, L_d^0, \mathcal{T}_d^0$	Initial number of equipment, line crews and tree crews at d
$\mathcal{P}_d^D, \mathcal{P}_\tau^{EI}$	Cost of staging depot d and ordering equipment τ
$\mathcal{P}_c^H, \mathcal{P}^{EC}$	Hourly pay for crew c and cost of obtaining an external crew
$\mathcal{P}_\tau^{LF}, \mathcal{P}^R$	Penalty costs for late delivery of equipment τ and penalty on restoration time
$\mathcal{P}_{d,e,\tau}^{TE}$	Cost of transporting equipment τ between locations d to e
$\mathcal{R}_{k,\tau,s}$	The number of type τ resources required to repair damaged line k in scenario s
$\mathcal{U}_{k,s}^T$	Binary random variable equals one if line k in scenario s is damaged by a tree
$\mathcal{U}_{k,s}^L$	Binary random variable indicating the damage state of line k in scenario s.

Decision Variables

$A_{k,c,s}^{L/T}$	Binary variable equal to 1 if line k is assigned to line/tree crew c in scenario s
$\delta_{d,c}$	Binary variable equals 1 if crew c is positioned in depot d
$E_{d,e,\tau}$	Number of τ supplies transferred between depots d and e
$E_{c,d,\tau,s}^C$	The amount of type τ supplies that crew c obtains from depot d in scenario s
$\mathcal{E}_{d,\tau,s}$	Additional τ supplies required in depot d scenario s
$EI_{d,\tau}, E_{d,\tau}^D$	Number of τ supplies ordered to depot d and the total number of τ supplies at d
$L_{d,e}, \mathcal{T}_{d,e}$	Number of line and tree crews transferred from depot d to e
$LI_d, \mathcal{T}I_d$	Number of external line and tree crews positioned at depot d

AQ1 Manuscript received March 11, 2019; revised June 3, 2019; accepted June 23, 2019. This work was supported in part by the U.S. Department of Energy's Solar Energy Technologies Office under Grant CPS4228, and in part by the National Science Foundation under Grant ECCS 1609080. Paper no. TSG-00367-2019. *(Corresponding author: Zhaoyu Wang.)*

A. Arif is with the Department of Electrical and Computer Engineering, Iowa State University, Ames, IA 50011 USA, and also with the Department of Electrical Engineering, King Saud University, Riyadh 11451, Saudi Arabia (e-mail: aiarif@iastate.edu).

Z. Wang is with the Department of Electrical and Computer Engineering, Iowa State University, Ames, IA 50011 USA (e-mail: wzy@iastate.edu).

C. Chen and B. Chen are with the Energy Systems Division, Argonne National Laboratory, Lemont, IL 60439 USA (e-mail: morningchen@anl.gov; bo.chen@anl.gov).

Color versions of one or more of the figures in this paper are available online at http://ieeexplore.ieee.org.

Digital Object Identifier 10.1109/TSG.2019.2925620

$\mathcal{L}_s^L, \mathcal{L}_s^T$	The expected times of the last repair conducted by the line and tree crews
$H_{c,s}$	Amount of hours crew c is expected to work in scenario s
v_d	Binary variable equals 1 if depot d is staged
u_k, y_i	Binary variables indicating the connection status of line k and load at bus i.

I. Introduction

Outages due to weather-related events cause significant damage to the power grid infrastructure. In 2017, around 37 million customers were affected by power outages in the United States [1]. This threat to the electric grid has raised a growing need to address disaster management and power system resilience. Disaster management consists of four phases: mitigation, preparedness, response, and recovery. For power systems, the mitigation and preparation phases include long-term and short-term pre-disaster planning. Tree trimming, pole hardening, and distributed generator (DG) installation belong to long-term pre-disaster planning [2]. Short-term pre-disaster planning includes acquiring and allocating crews and equipment and selecting staging areas. The response and recovery phases are post-disaster actions that include damage assessment [3], crew dispatch and repair scheduling, and service restoration [4]. Effective disaster management measures can improve power system resistance during extreme events and accelerate recovery after events. The focus of this paper is to study the short-term pre-disaster preparation problem, which is critical to achieve resiliency. Resilience is defined as the ability to prepare for, adapt to, withstand, and recover rapidly from disruptions [5]. Pre-disaster planning enables efficient post-disaster recovery by ensuring there are enough and optimal number of equipment and crews in the right places to quickly conduct the repairs [6].

After severe events, utility companies dispatch emergency crews to assess and repair the damage in order to restore power as fast as possible. A major challenge that utilities face is the lack of resources, including human resources and equipment, to handle extreme events [7]. Once utilities request assistance from neighboring companies, they are facing another task of managing the newly acquired resources. Utilities must provide water, food, and shelter [8] and communicate differences in work practices to the visiting crews [6]. For these reasons, early preparation is essential to deal with upcoming extreme or severe weather events. This paper aims to develop a method to assist utilities in their preparation process by identifying the required resources and preallocating the crews and equipment.

Disaster preparation is a well-studied research area [9]–[15]. In [9], a two-stage stochastic programming model was developed to select the storage location of medical supplies, and the required amount of various supplies before a disaster. The objective of the developed model was to minimize the operation cost of the warehouses, the total transportation time, and the unfulfilled demand. A similar stochastic problem was tackled in [10], while considering the impact of the disaster on the warehouses. The paper used Benders Decomposition to solve the stochastic model. The authors in [11] developed a multi-objective mixed integer linear program (MILP) to determine the location of emergency facilities, resource allocation and relief distribution for flood preparation. The authors in [12] used robust optimization to produce a logistic plan for mitigating demand uncertainty in humanitarian relief supply chains. A multi-objective robust model for humanitarian relief logistics was developed in [13]. The paper considered demand and supply uncertainty and considered the possibility that some supplies may be damaged during the event. In [14], the authors developed a p-robust optimization model, which combines robust optimization with Monte Carlo simulation, for determining the location of relief bases, number of rescue vehicles, and other relief supplies. A min-max robust model is developed in [15] to optimize the relief facility location and pre-position emergency supplies for disaster preparation.

However, further research is needed on disaster preparation in the context of power system and its infrastructure. In [16], the authors divided the power network into different areas/cells, and developed a MILP to find the optimal number of depots and their locations. Each area was assumed to have a specific demand and can only contain one depot. The objective was to minimize the transportation cost between the predefined areas. A storage and customer allocation problem was presented in [17]. The authors developed a multi-objective stochastic mixed-integer program (SMIP) that determines which warehouse to use and the number of resources to store in each warehouse. The objectives were to minimize the amount of unsatisfied demand, the transportation cost of the resources between the warehouses, and the investments and maintenance cost of the warehouses. Reference [18] developed a SMIP model and a column generation approach for stockpiling resources before a disaster. The developed approach focused on determining the quantity and type of equipment, while neglecting the crews and the distances between the warehouses and the damaged components.

The distribution system preparation problem is a challenging one because it combines the combinatorial optimization problems of depot location, equipment transportation and allocation, and crew allocation. The preparation problem is inherently stochastic, as the damaged components and the required resources are not known beforehand. This makes it a complex stochastic combinatorial optimization problem. The previous work approached the preparation stage by dividing the electric network into different areas, with each area having a specific demand. This kind of approach neglects the individual components within each area and the distances between these components and the depots. Moreover, the interdependence between the location and number of crews, damaged components in the network, and the number of resources required to repair the damage was not examined in the preparation stage. We propose a two-stage SMIP to model the preparation problem. The first stage in the stochastic program is to determine the depots and the locations of crews and equipment. The second stage is the recourse action that deals with acquiring new equipment and assigning the crews to repair the damaged components. The contributions of this paper are listed as follows:

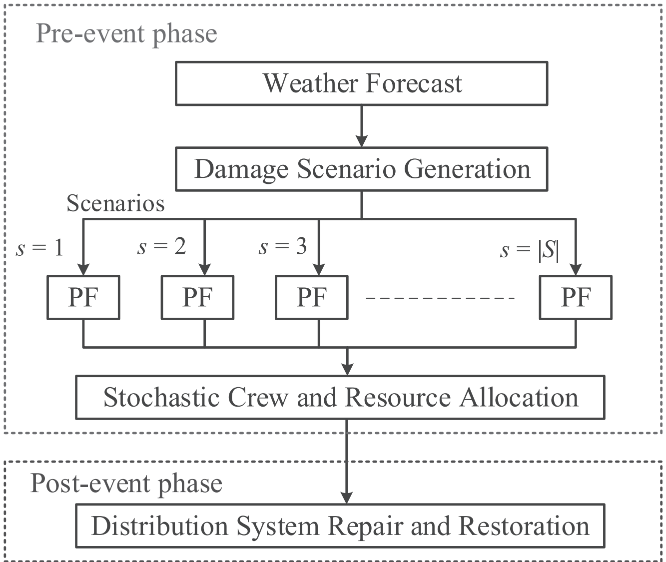

Fig. 1. Framework for extreme event proactive recovery operation.

- A new two-stage SMIP model is developed and used to select depots and allocate crews and equipment. We consider different types of crews (line and tree crews) and equipment (poles, transformers, and conductor). The stochastic problem is solved using a modified Progressive Hedging algorithm and high performance computing.
- Mathematical equations for modeling the interdependencies of the depots, crews, equipment, and damaged components are formulated. Also, symmetry-breaking constraints are designed to improve the performance of the model.
- We provide a procedure for estimating the number and types of required equipment after extreme weather events, in addition to identifying the critical components to repair.

The rest of the paper is organized as follows. Section II presents the framework of this paper. Outage scenario generation is discussed in Section III. The formulation for prepositioning the crews and allocating the resources is presented in Section IV. The simulation and results are presented in Section VI and Section VII concludes this paper.

II. Framework

Extreme weather events result in damage to the electric grid infrastructure, which leads to significant losses and power outages. Utilities mobilize the available crews to damage sites to repair the damaged components and restore normal operation. The effectiveness of the recovery response depends on the preparation processes that are taken before extreme events hit. For an upcoming severe weather event, utilities position repair crews and supplies in (or near) the areas that are expected to suffer the greatest damage. In addition, utilities can acquire services from crews in neighboring utilities through mutual assistance programs. Pre-staging crews, equipment and other resources safely before a severe event allows for a proactive response and efficient resource management. Fig. 1 illustrates the proposed pre- and post-event framework.

First, the forecasted weather and fragility models of the components are used to generate damage scenarios. For each scenario, we solve a power flow (PF) problem to identify critical components that must be repaired to restore service for high-priority customers. This information is used in the stochastic crew and resource allocation problem (SCRAP) to ensure there is enough equipment to repair the critical components. Once the weather event hits the distribution system, the repair and restoration problem is solved to restore the network to its normal state [19]–[21]. This paper focuses on the steps before the weather event occurs.

III. Damage Scenario Generation

Prepositioning crews and resources is subject to uncertain damage states of distribution lines. In this paper, the uncertainty is represented by a finite set of discrete scenarios, which are obtained using a Monte Carlo sampling procedure. The Monte Carlo sampling method generates $|S|$ number of scenarios with equal probability ($1/|S|$). The focus of this paper is on the impact of strong wind events, such as hurricanes and windstorms. Since the study focuses on wind-related failures, we only consider overhead distribution lines. To generate damage scenarios, we first estimate the wind speed that will affect the distribution system. In this paper, we simulate hurricane events for illustration.

A. Hurricane Model

Since distribution networks cover small geographical areas, we assume that the wind speed experienced by all components in a distribution network is the same at any given moment [22]. The wind speed $w(t, s)$ that impacts the distribution network at time t and scenario s is modeled using the inland wind decay model [23], which is expressed by the following equation:

$$w(t, s) = w_b + \left(R_w w_s^0 - w_b\right) e^{-\alpha_w t} - C_w \qquad (1)$$

where w_s^0 is the maximum sustained surface wind speed at landfall in scenario s; $\alpha_w = 0.095\text{h}^{-1}$ is the decay constant; $w_b = 26.7$ knots (kt) is the background wind speed; and $R_w = 0.9$ is a reduction factor that represents the abrupt wind speed decrease as hurricanes make landfall. In this paper, the value of w_s^0 is simulated using a logonormal distribution to generate the scenarios. C_w is a factor that represents the effect of the distance inland [23].

B. Fragility Models

Distribution lines are modeled using edges that connect distribution buses, which connect customers to the distribution network. Distribution lines include poles and conductors between the poles. Damage of a single pole or conductor on a distribution line renders the line inoperable. Therefore, we conduct fragility analysis for each pole and conductor in the system, while assuming that the fragility of different components is independent.

1) Pole Failure: Using the fragility model presented in [25], the probability of failure for pole z is found using the following equation:

$$p_z^p(w) = \min\{a^p e^{b^p w}, 1\} \tag{2}$$

where a^p and b^p are constants related to pole properties, and w is the wind speed.

2) Conductor Failure: Conductors between distribution poles are prone to failures due to strong winds and falling trees during severe events [25]. Define p_l^w as the direct wind-induced damage probability, and p_l^t as the damage probability due to a fallen tree near conductor l [22], [26]. The wind-induced damage probability of a conductor is calculated using the ratio of the maximum perpendicular force that the conductor can endure F_l^f and the conductor wind loading F_l^w [26]. The wind loading and p_l^w are calculated by [27]:

$$q_l(w) = 0.613(G_1 G_2 G_3 w)^2 \tag{3}$$

$$F_l^w(w) = L_l^c \times D_l^c \times q_l(w) \times C^f \tag{4}$$

$$p_l^w(w) = \min\left\{F_l^w(w)/F_l^f, 1\right\} \tag{5}$$

Equation (3) calculates the dynamic pressure $q_l(w)$ (N/m^2), where G_1, G_2, and G_3 are factors related to the topography, ground roughness, and a statistical factor depending upon level of security required. L_l^c is the length (m) and D_l^c is the diameter (m) of conductor l, and C^f is a force coefficient [27]. As for the damage due to fallen trees, the probability is modeled by [28]:

$$p_l^t(w) = \frac{e^{h(S_l^w)}}{1 + e^{h(S_l^w)}} \tag{6}$$

$$h(S_l^w) = a_h + c_h(k_l S_l^w) D_H^{b_h} \tag{7}$$

where a_h, b_h, and c_h are parameters associated with tree species, S_l^w is the estimated storm severity on conductor l (which varies from 0-1), k_l is a factor that represents the local terrain effects, and D_H is the tree diameter at breast height.

C. Equipment

The damage state of a component is determined using Bernoulli distribution (Bernoulli(p)), which takes the value of 1 (damaged) with probability p, and 0 (functional) with probability $1 - p$. For each scenario, we evaluate the status of the system using the maximum sustained wind speed $\bar{w}_s = max_{\forall t}\{w(t, s)\}, \forall s$. Therefore, the damage state of pole z in scenario s is determined by the outcome of the random variable $\psi_{z,s}^{pole} \sim$ Bernoulli($p_z^p(\bar{w}_s)$). A conductor can either be damaged by wind force $\psi_{l,s}^{wind} \sim$ Bernoulli($p_l^w(\bar{w}_s)$) or tree $\psi_{l,s}^{tree} \sim$ Bernoulli($p_l^t(\bar{w}_s)$). Consequently, the damage state of conductor l is determined as $\psi_{l,s}^{cond} = \psi_{l,s}^{wind} \vee \psi_{l,s}^{tree}$. After assessing the state of damage for each conductor and pole in the network, we can estimate the amount and type of equipment required to repair the damaged components. Although distribution networks include many types of components, we classify them into the following categories:

- Type 1: Poles for 3-phase lines
- Type 2: Poles for 1- and 2-phase lines
- Type 3: 3-phase transformers with protective equipment
- Type 4: 1-phase transformers with protective equipment
- Type 5: Conductors

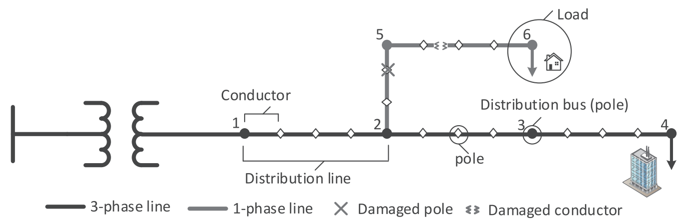

Fig. 2. Single line diagram of a distribution network. AQ2

The line segment connecting two distribution buses consists of poles and conductors, as shown in Fig. 2, where line 2–5 has one damaged pole and line 5–6 has one damaged conductor. In case of a damaged bus, such as bus 3 in Fig. 2, both lines 2–3 and 3–4 are affected. To avoid repetition when calculating the number of equipment required and repair time, we associate the poles on shared buses (e.g., pole at bus 3 for lines 2–3 and 3–4) with the line that has the bus with the lowest index (line 2–3). The number of type τ equipment required for line k in scenario s can be calculated using the following equations:

$$\mathcal{R}_{k,\tau,s} = \sum_{z \in \Omega_L^p(k,\tau)} \psi_{z,s}^{pole}, \ \forall k, \tau \in \{1 \ldots 4\}, s \tag{8}$$

$$\mathcal{R}_{k,5,s} = n_k^\phi L_l^c \sum_{l \in \Omega_L^c(k)} \psi_{l,s}^{cond}, \ \forall k, s \tag{9}$$

where $\Omega_L^p(k, \tau)$ is the set of type τ equipment for the poles on line k, $\Omega_L^c(k)$ is the set of conductors on line k, and n_k^ϕ is the number of phases for line k. Equation (8) calculates the number of pole-related equipment and (9) calculates the amount of conductor required.

D. Repair Time

The repair times for the damaged lines are estimated based on the number of damaged conductors and poles. The repair time for a damaged distribution pole is assumed to satisfy a normal distribution with mean 5 hours and 2.5 hours standard deviation ($r_{z,s}^p \sim \mathcal{N}(5, 2.5)$) [25]. For damaged conductors, the repair time is assumed to satisfy a normal distribution with mean 4 hours and 2 hours standard deviation ($r_{l,s}^c \sim \mathcal{N}(4, 2)$) [25]. The estimated time to repair a damaged line is found by adding the repair times of the damaged poles and conductors of the line, as follows:

$$ET_{k,s}^L = \sum_{z \in \Omega_L^p(k)} \psi_{z,s}^{pole} \ r_{z,s}^p + \sum_{l \in \Omega_L^c(k)} \psi_{l,s}^{cond} \ r_{l,s}^c, \ \forall k, s \tag{10}$$

According to the report in [29], the average time to remove a tree after a storm is 1 hour. Therefore, the tree removal time for each line, in hours, is estimated by calculating the number of downed trees on the line:

$$ET_{k,s}^T = \sum_{l \in \Omega_L^c(k)} \psi_{l,s}^{tree}, \ \forall k, s. \tag{11}$$

E. Critical Components

After extreme events cause large-scale outages, it is imperative to quickly restore power to critical sites, such as hospitals, community shelters and emergency dispatch centers.

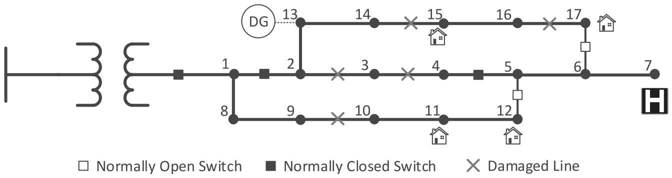

Fig. 3. Single line diagram of a distribution network.

Therefore, we must ensure that there are enough equipment and resources to repair vulnerable lines near critical sites. A MILP model is used to solve a PF problem to determine the critical lines to be repaired, so that all critical loads are restored. If one pole or conductor on a line is damaged, then the whole line is considered to be damaged and cannot be operated. The binary variable $\mathcal{U}_{k,s}^{L}$ is used to indicate the damage state of line k, $\mathcal{U}_{k,s}^{L} = 1$ if $\psi_{z,s}^{pole} = 1$ or $\psi_{l,s}^{cond} = 1$ for any $(i, l) \in k$. For example, both lines 2–5 and 5–6 are damaged in Fig. 2, therefore, $\mathcal{U}_{2-5}^{L} = \mathcal{U}_{5-6}^{L} = 1$. The set of damaged lines $\Omega_{DL}(s)$ can the be found by using the binary variable $\mathcal{U}_{k,s}^{L}$, such that $\Omega_{DL}(s) = \{k|\mathcal{U}_{k,s}^{L} = 1, \forall k, s\}$. Define binary variables u_k which equals 1 if line k is repaired and 0 otherwise, and y_i as the connection status of load at bus i. The MILP for identifying the critical components is formulated as follows:

$$\min \sum_{k \in \Omega_{DL}(s)} u_k \tag{12}$$

$$\text{subject to } \; y_i = 1, \;\; \forall i \in \Omega_{CD} \tag{13}$$

subject to power operation constraints [21] where Ω_{CD} is the set of buses with critical loads. In this paper, we provide a summary for the model due to space limitations. The objective (12) minimizes the number of lines to repair. Constraint (13) indicates that all critical loads must be served. Furthermore, power operation constraints such as power flow, network reconfiguration, fault isolation, and distributed generator (DG) dispatch are used in the model [21]. Consider the distribution network shown in Fig. 3, with a critical load located at bus 7, and 5 damaged lines. In order to restore the load at bus 7 with minimal repairs, line 9–10 must be repaired ($u_{9-10} = 1$), switch 5–12 closed, and switches 1–2 and 4–5 opened to keep the damaged lines isolated. If line 9–10 requires 2 poles to repair, then the utility must have a minimum of 2 poles in their inventory. The PF model is solved for each generated scenario s. The set of critical lines $\Omega_{CL}(s)$ for scenario s can then be found as: $\Omega_{CL}(s) = \{k|u_k = 1, \forall k \in \Omega_{DL}(s), s\}$. This information is used in the SCRAP model in the following section.

IV. STOCHASTIC CREW AND RESOURCE ALLOCATION

The decision variables in the two-stage crew and resource allocation problem can be divided into two groups. The first group is the first-stage variables that are determined before the realization of the uncertain parameters. These variables include the number of external equipment and crews ($EI_d, LI_d, \mathcal{T}I_d$), the number of equipment and internal crews transferred between depots d and e ($E_{d,e,\tau}, L_{d,e}, \mathcal{T}_{d,e}$), and the number of equipment in each depot d ($E_{d,\tau}^{D}$). Furthermore, a

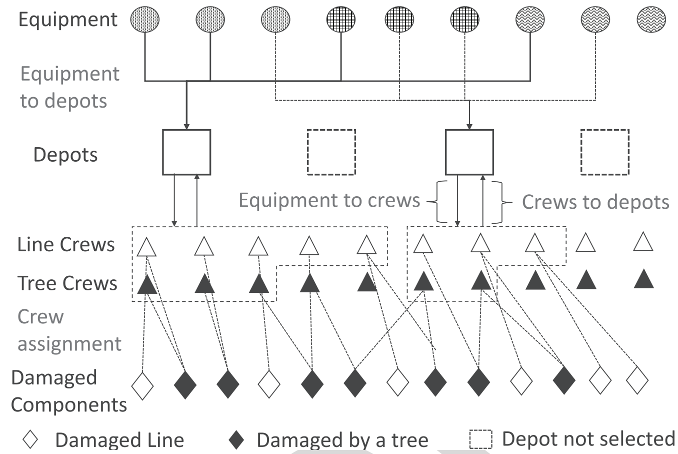

Fig. 4. Crew and equipment allocation.

decision on utilizing a depot is made in the first stage using binary variable (ν_d), while the location of each crew is determined using binary variable ($\delta_{d,c}$). The second part contains the second-stage variables, which are decided according to specific realization of the uncertainty. The second-stage variables are indexed by s to indicate the response for the specific scenario. In this stage, the crews are assigned to damaged lines ($A_{k,c,s}^{L}, A_{k,c,s}^{T}$) to ensure they are staged near the damaged lines, and the expected working hours for each crew ($H_{c,s}$) is estimated. Also, the number of additional equipment required ($\mathcal{E}_{d,\tau,s}$) to finish the repairs is determined in this stage. SCRAP models a joint location-allocation-inventory problem. Fig. 4 provides an illustration for the SCRAP model, which includes the following steps: 1) depots are selected; 2) different types of equipment are allocated to depots; 3) line and tree crews are allocated to the depots; 4) equipment is assigned to crews; and 5) crews are assigned to damaged components. The two-stage stochastic crew and resource allocation problem is formulated in the following subsections.

A. Objective

$$\begin{aligned}
\min & \sum_{\forall d,e,\tau} \mathcal{P}_{d,e,\tau}^{TE} E_{d,e,\tau} + \sum_{\forall d,\tau} \mathcal{P}_{\tau}^{EI} EI_{d,\tau} \\
& + \sum_{\forall d} \Big(\mathcal{P}^{EC} (LI_d + \mathcal{T}I_d) + \mathcal{P}_d^{D} \nu_d \Big) \\
& + \sum_{\forall s} \Pr(s) \left(\sum_{\forall c} \mathcal{P}_c^{H} H_{c,s} + \sum_{\forall d,\tau} \mathcal{P}_{\tau}^{LF} \mathcal{E}_{d,\tau,s} + \mathcal{P}^{R} \big(\mathcal{L}_s^{T} + \mathcal{L}_s^{L} \big) \right)
\end{aligned} \tag{14}$$

The first two lines in (14) are for the first-stage objective, which aims to minimize the costs of equipment transportation, ordering equipment and external crews, and staging depots. The third line in (14) is dependent on the realization of the uncertainty, i.e., the second-stage objective. The first term in the second-stage objective minimizes the labor costs associated with the crews. The second and third terms are penalty costs. We add a penalty cost for unmet equipment demand and penalize the time needed to repair all components. The penalty $\mathcal{P}_{\tau}^{LF}$ minimizes the shortage of equipment. The purpose of penalizing the expected time of the last repair is to minimize the system restoration time.

B. First-Stage Constraints

In the first stage, the depots are selected and both equipment and crews are allocated to the selected depots in anticipation of an extreme event. Constraints (15)-(22) represent the first-stage constraints.

1) Depot Selection:

$$1 \leq \sum_{\forall d} \nu_d \leq \nu^{max} \tag{15}$$

$$0 \leq \sum_{\forall \tau} \mathcal{C}_{\tau}^{R} E_{d,\tau}^{D} \leq \mathcal{C}_{d}^{E} \nu_d, \ \forall d \tag{16}$$

$$0 \leq \sum_{\forall c} \delta_{d,c} \leq \mathcal{C}_{d}^{H} \nu_d, \ \forall d \tag{17}$$

The number of selected depots is limited to ν^{max} in (15), and at least one depot must be selected. Each depot, if selected, can contain a limited amount of equipment, as enforced by (16). Constraint (17) limits the number of crews in depots. A depot can accommodate a limited number of crews depending on its resources. The limits in (16) and (17) are multiplied by ν_d so that if the depot is not selected, it will have no crew or equipment.

2) Crew and Equipment Allocation:

$$E_{d,\tau}^{D} = E_{d,\tau}^{0} + \sum_{\forall e, e \neq d} E_{e,d,\tau} - \sum_{\forall e, e \neq d} E_{d,e,\tau} + EI_{d,\tau}, \ \forall d, \tau \tag{18}$$

$$\sum_{\forall c \in C^L} \delta_{d,c} = L_d^0 + \sum_{\forall e, e \neq d} L_{e,d} - \sum_{\forall e, e \neq d} L_{d,e} + LI_d, \ \forall d \tag{19}$$

$$\sum_{\forall c \in C^T} \delta_{d,c} = \mathcal{T}_d^0 + \sum_{\forall e, e \neq d} \mathcal{T}_{e,d} - \sum_{\forall e, e \neq d} \mathcal{T}_{d,e} + \mathcal{T}I_d, \ \forall d \tag{20}$$

$$\sum_{\forall d} \delta_{d,c} = 1, \ \forall c \in IC \tag{21}$$

$$\sum_{\forall d} \delta_{d,c} \leq 1, \ \forall c \notin IC \tag{22}$$

Constraints (18)-(20) model the transportation of equipment, line crews, and tree crews, respectively. The three constraints are formulated using flow conservation equations. For instance, the constraint for the equipment (18) states that the amount of type τ equipment in depot d is equal to the sum of equipment initially in the depot, equipment transferred to the depot, newly obtained equipment, and minus the equipment transferred to other depots. The summations $\sum_{\forall c \in C^L} \delta_{d,c}$ and $\sum_{\forall c \in C^T} \delta_{d,c}$ are the number of line and tree crews in depot d, respectively. The first term in the right-hand side of (19) is the number of line crews initially present in depot d. The second term represents the number of line crews transferred to depot d and the third term is the number of line crews transferred from depot d. The last term LI_d is the number of visiting line crews to be positioned in depot d. Similarly, constraint (20) is designed for tree crews. Constraint (21) states that each internal crew must be located in one of the depots, while external crews can be either located in one depot, or not used; i.e., $\delta_{d,c} = 0$, as enforced by (22).

3) Symmetry-Breaking Constraints: The presented problem allow a large number of feasible symmetric solutions with equal objective value. Therefore, we add symmetry breaking constraints to keep at least one solution and remove all other symmetric solutions. Consider a case where there are four line crews and three potential depots. Assume that depot 1 and depot 3 are selected, and all four crews must be allocated. In this case, there are four possible solutions for allocating the crews:

$$\delta_{d,c} = \begin{pmatrix} 1 & 1 & 0 & 0 \\ 0 & 0 & 0 & 0 \\ 0 & 0 & 1 & 1 \end{pmatrix} \equiv \begin{pmatrix} 1 & 0 & 1 & 0 \\ 0 & 0 & 0 & 0 \\ 0 & 1 & 0 & 1 \end{pmatrix} \equiv \begin{pmatrix} 0 & 1 & 0 & 1 \\ 0 & 0 & 0 & 0 \\ 1 & 0 & 1 & 0 \end{pmatrix}$$

$$\equiv \begin{pmatrix} 0 & 0 & 1 & 1 \\ 0 & 0 & 0 & 0 \\ 1 & 1 & 0 & 0 \end{pmatrix} \tag{23}$$

To deal with the symmetry problem in (23), we allocate the crews to the depot starting from the lowest indexed row and column. Therefore, for $\delta_{d,c} = 1$, all depots with indices $\bar{d} < d$ must not have any crews with indices $\bar{c} > c$, i.e., $\delta_{\bar{d},\bar{c}} = 0$. The following equations are used to break the symmetry in (23):

$$\sum_{\forall d} \delta_{d,c+1} \geq \sum_{\forall d} \delta_{d,c}, \forall c \in C^L, \ c < |C^L| \tag{24}$$

$$\sum_{\forall d} (|\Omega_P| - d) \delta_{d,c+1} \geq \sum_{\forall d} (|\Omega_P| - d) \delta_{d,c}, \ \forall c \in C^L, c < |C^L| \tag{25}$$

$$\sum_{\forall d} \delta_{d,c+1} \geq \sum_{\forall d} \delta_{d,c}, \forall c \in C^T, \ c < |C^T| \tag{26}$$

$$\sum_{\forall d} (|\Omega_P| - d) \delta_{d,c+1} \geq \sum_{\forall d} (|\Omega_P| - d) \delta_{d,c}, \ \forall c \in C^T, \ c < |C^T| \tag{27}$$

Constraint (24) state that for similar crews, we allocate the crew with the lowest index first. Constraint (25) allocates the crews starting from the depots with the lowest index, and skips depots that are not staged. Constraints (24) and (25) are also enforced to the tree crews in (26) and (27). The feasible solutions are then reduced from four to one possible solution in this example, where only the first matrix in (23) is feasible.

C. Second Stage Constraints

After selecting the depots and allocating the crews and equipment in the first stage, the crews are assigned to repair the damaged components and the equipment are distributed to the crews in the second stage.

1) Crew Assignment:

$$\sum_{\forall c \in C^L} A_{k,c,s}^{L} = \mathcal{U}_{k,s}^{L}, \ \forall k, s \tag{28}$$

$$\sum_{\forall c \in C^T} A_{k,c,s}^{T} = \mathcal{U}_{k,s}^{T}, \ \forall k, s \tag{29}$$

$$\sum_{\forall k} A_{k,c,s}^{L} \leq M \sum_{\forall d} \delta_{d,c}, \ \forall c \in C^L, s \tag{30}$$

$$\sum_{\forall k} A_{k,c,s}^{T} \leq M \sum_{\forall d} \delta_{d,c}, \ \forall c \in C^T, s \tag{31}$$

$$\bar{D} \geq D_{d,k}\big(\delta_{d,c} + A^L_{k,c,s} - 1\big),\ \forall d, k, c \in C^L, s \quad (32)$$

$$\bar{D} \geq D_{d,k}\big(\delta_{d,c} + A^T_{k,c,s} - 1\big),\ \forall d, k, c \in C^T, s \quad (33)$$

Equations (28) and (29) assign the line and tree crews to the damaged lines, respectively. The binary parameter $\mathcal{U}^T_{k,s}$ equals 1 (0) if line k is damaged (functional). Therefore, if $\mathcal{U}^L_{k,s}$ equals 0, then line k will not be assigned to any crews (i.e., $\sum_{\forall c \in C^L} A^L_{k,c,s} = 0$). Also, if crew c is not staged at a depot (i.e., $\sum_{\forall d} \delta_{d,c} = 0$), then crew c is not assigned to any damaged line as enforced by (30) and (31). The big M value in (30) can be the maximum number of damaged lines ($\max_{\forall s}(\sum_{\forall k} \mathcal{U}^L_{k,s})$). Constraints (32)-(33) are used to identify the distances between the damaged components assigned to each crew and the depots. This distance is limited to $\bar{D}$. If line crew c is positioned at depot d ($\delta_{d,c} = 1$) and is assigned to line k ($A^L_{k,c,s} = 1$), then $\bar{D} \geq D_{d,k}$.

2) Working Hours: In this subsection, we estimate the working hours for each crew in order to distribute the working assignments fairly between the crews and ensure that enough crews are present. The working hours constraints are modeled in (34)-(37).

$$H_{c,s} = \sum_{\forall k}(ET^L_{k,s} A^L_{k,c,s}),\ \forall c \in C^L, s \quad (34)$$

$$H_{c,s} = \sum_{\forall k}\big(ET^T_{k,s} A^T_{k,c,s}\big),\ \forall c \in C^T, s \quad (35)$$

$$\mathcal{L}^L_s \geq H_{c,s},\ \forall c \in C^L, s \quad (36)$$

$$\mathcal{L}^T_s \geq H_{c,s},\ \forall c \in C^T, s \quad (37)$$

The total expected working time for each line and tree crew is calculated in (34) and (35). Constraints (36) and (37) define the expected time of the last repair. The value of $\mathcal{L}^L_s$ is greater or equal to the largest $H_{c,s}$ for the line crews, and $\mathcal{L}^T_s$ is greater or equal to the largest $H_{c,s}$ for the tree crews. Since we are minimizing the expected time of the last repair, it will take the value $max_{\forall c}(H_{c,s})$ in each scenario. By minimizing $\mathcal{L}^L_s$ and $\mathcal{L}^T_s$, we minimize the restoration time of the system and ensure that we do not have a single crew or few crews in a location with many damaged components.

3) Equipment Assignment: The next set of constraints model the distribution of equipment to the depots and crews.

$$\sum_{\forall d} E^D_{d,\tau} \geq \sum_{\forall k \in \Omega_{CL}(s)} \mathcal{R}_{k,\tau,s},\ \forall \tau, s \quad (38)$$

$$\sum_{\forall d}\big(E^D_{d,\tau} + \mathcal{E}_{d,\tau,s}\big) \geq \sum_{\forall k} \mathcal{R}_{k,\tau,s},\ \forall \tau, s \quad (39)$$

$$\sum_{\forall \tau} E^C_{c,d,\tau,s} \leq M\delta_{d,c},\ \forall d, c \in C^L, s \quad (40)$$

$$\sum_{\forall c \in C^L} E^C_{c,d,\tau,s} \leq E^D_{d,\tau} + \mathcal{E}_{d,\tau,s},\ \forall d, \tau, s \quad (41)$$

$$\sum_{\forall d} E^C_{c,d,\tau,s} \geq \sum_{\forall k} A^L_{k,c,s} \mathcal{R}_{k,\tau,s},\ \forall c \in C^L, \tau, s \quad (42)$$

Constraint (38) indicates that the number of equipment available must be sufficient for repairing all critical lines before the extreme event occurs. Constraint (39) states that the total equipment that the utility have must be equal or greater than the required equipment to repair the damaged components. $\mathcal{E}_{d,\tau,s}$ identifies the additional number of equipment (unmet equipment demand) that must be ordered in each scenario to finish the repairs. Each crew can obtain equipment from the depot they are positioned at, as enforced by constraint (40). The crews must use the resources available in the depot (41). Constraint (42) indicates that the number of resources the crew have should be enough to repair the assigned damaged components. After positioning the crews and resources, the utility will be ready for the recovery operation after the outages. The next section presents the algorithm used to solve the stochastic model.

V. Solution Algorithm

The standard method for solving stochastic programs is to use a MILP solver, e.g., CPLEX, to directly solve the extensive form (EF) of the SMIP. Define ($\boldsymbol{x}$) and ($\boldsymbol{y_s}$) as vectors containing the first-stage and second-stage variables, respectively. Also, let $\boldsymbol{a}$ and $\boldsymbol{b_s}$ represent the coefficients associated with ($\boldsymbol{x}$) and ($\boldsymbol{y_s}$), then the EF form of the SMIP can be expressed as follows:

$$\zeta = \min_{\boldsymbol{x},\boldsymbol{y_s}}\ \boldsymbol{a}^T\boldsymbol{x} + \sum_{\forall s} \mathrm{Pr(s)}\ \boldsymbol{b_s}^T\boldsymbol{y_s} \quad (43)$$

$$\text{s.t.}\ \ (\boldsymbol{x}, \boldsymbol{y_s}) \in \mathcal{Q}_s,\ \forall s \quad (44)$$

where $(\boldsymbol{x}, \boldsymbol{y_s}) \in \mathcal{Q}_s$ represents the subproblem constraints that ensures a feasible solution. Solving the EF for large-scale problems is however computationally difficult. Decomposition methods, such as the L-shaped and Benders Decomposition methods [30], have been proposed in the literature to solve stochastic programs. The L-shaped method and Benders decomposition cannot be applied directly when the second stage is non-convex with integer values, which is the case for the preparation problem in this paper. Rockafellar and Wets developed the Progressive Hedging (PH) algorithm as a heuristic to effectively solve SMIP problems [31]. The algorithm decomposes the EF into scenario-based subproblems. Therefore, for $|\mathcal{S}|$ scenarios, the SMIP is decomposed into $|\mathcal{S}|$ subproblems. The PH algorithm is described in Algorithm 1.

The first step initializes the iteration number τ and the individual scenarios are solved in Step 2. In Step 3, the first stage solution obtained from Step 2 is aggregated. Step 4 calculates the multiplier η_s. The multiplier is used in Step 6 to update $\boldsymbol{x}$, where the scenarios are solved independently in parallel. Steps 7 and 8 update the first-stage solution and the multiplier, respectively. The program terminates once all first-stage decisions $\boldsymbol{x_s}$ converge to the same $\bar{\boldsymbol{x}}$ in Step 9, i.e., $\sum_{s \in \mathcal{S}} \mathrm{Pr(s)}||\boldsymbol{x_s}^{(\tau)} - \bar{\boldsymbol{x}}^{(\tau)}|| < \varepsilon$. The PH algorithm may experience slow convergence with large problems that include many scenarios. A detailed analysis of PH showed that individual first-stage variables frequently converge to specific values across all scenario subproblems [32]. Therefore, we fix some of the first-stage variables if they converge to the same values after certain numbers of iterations. In the SCRAP model, we fix the variable ν_d (depot selected) if it converges to the same values after τ_1 iterations, as shown in Steps 12–16. In Steps 17–21, the crew allocation and selection variable $\delta_{d,c}$ is fixed after τ_2 iterations if the variable converges to the same

Algorithm 1 The Two-Stage PH Algorithm

1: Let $\tau := 0$
2: For all $s \in \mathcal{S}$, compute:
$\boldsymbol{x_s}^{(\tau)} := \arg\min_{\boldsymbol{x}} \left\{ \boldsymbol{a}^T \boldsymbol{x} + \boldsymbol{b_s}^T \boldsymbol{y_s} \,:\, (\boldsymbol{x}, \boldsymbol{y_s}) \in \mathcal{Q}_s \right\}$
3: $\bar{\boldsymbol{x}}^{(\tau)} := \sum_{s \in \mathcal{S}} \Pr(\mathrm{s}) \boldsymbol{x_s}^{(\tau)}$
4: $\boldsymbol{\eta_s}^{(\tau)} := \rho(\boldsymbol{x_s}^{(\tau)} - \bar{\boldsymbol{x}}^{(\tau)})$
5: $\tau := \tau + 1$
6: For all $s \in \mathcal{S}$ compute:
$\boldsymbol{x_s}^{(\tau)} := \arg\min_{\boldsymbol{x}} \left\{ \boldsymbol{a}^T \boldsymbol{x} + \boldsymbol{b_s}^T \boldsymbol{y_s} + \boldsymbol{\eta_s}^{(\tau-1)} \boldsymbol{x} + \frac{\rho}{2} || \boldsymbol{x} - \bar{\boldsymbol{x}}^{(\tau-1)} ||^2 : (\boldsymbol{x}, \boldsymbol{y_s}) \in \mathcal{Q}_s \right\}$
7: $\bar{\boldsymbol{x}}^{(\tau)} := \sum_{s \in \mathcal{S}} \Pr(\mathrm{s}) \boldsymbol{x_s}^{(\tau)}$
8: $\boldsymbol{\eta_s}^{(\tau)} := \boldsymbol{\eta_s}^{(\tau-1)} + \rho(\boldsymbol{x_s}^{(\tau)} - \bar{\boldsymbol{x}}^{(\tau)})$
9: **if** $\sum_{s \in \mathcal{S}} \Pr(\mathrm{s}) || \boldsymbol{x_s}^{(\tau)} - \bar{\boldsymbol{x}}^{(\tau)} || < \varepsilon$ **then**
10: terminate
11: **else**
12: **if** $\tau \geq \tau_1$ **then**
13: **if** $\nu_{d,1}^{\tau} = \nu_{d,s}^{\tau}, \forall d, s$ **then**
14: **fix** $\nu_d = \nu_{d,s}^{\tau}, \forall d, s$
15: **end if**
16: **end if**
17: **if** $\tau \geq \tau_2$ **then**
18: **if** $\delta_{d,c,1}^{\tau} = \delta_{d,c,s}^{\tau}, \forall d, c, s$ **then**
19: **fix** $\delta_{d,c} = \delta_{d,c,s}^{\tau}, \forall d, c, s$
20: **end if**
21: **end if**
22: go to **Step 5**
23: **end if**

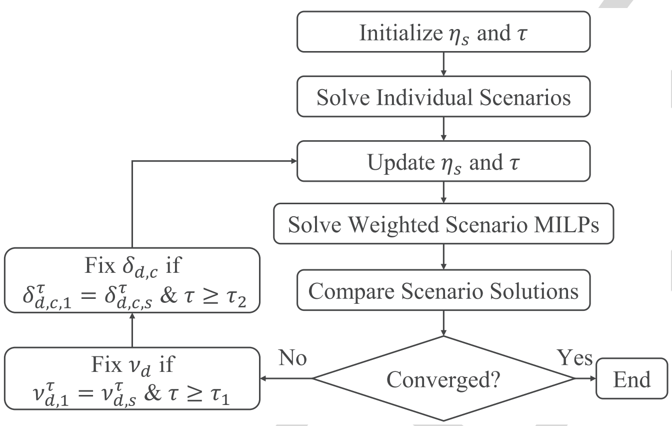

Fig. 5. Flowchart for the proposed PH algorithm.

value across all scenario subproblems. Once the variables are fixed, they are treated as parameters in the following iterations. In this paper, the values of τ_1 and τ_2 are set to be 5 and 20, respectively. A flowchart for the algorithm is given in Fig. 5.

VI. Simulation and Results

The preallocation model is simulated on the modified IEEE 123-bus distribution feeder [21], [33]. The size of the IEEE 123-bus feeder is scaled up, as shown in Fig. 6. The modified network, shown in Fig. 7, includes 4 dispatchable DGs, 18 new switches, 5 PVs and 2 battery energy storages. Note that Fig. 7 does not reflect the actual x- and y-coordinates. The 4 DGs are rated at 300 kW and 250 kVAr. The PV at bus 62 is rated at 900 kW and the other PVs are rated at 50 kW. The battery systems at bus 2 and 62 are rated at 50 kW/132 kWh

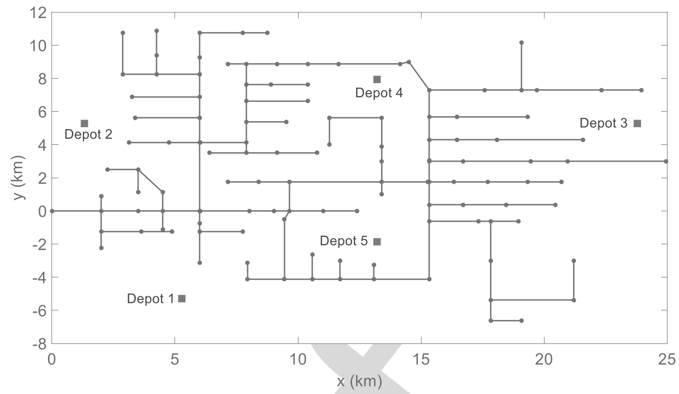

Fig. 6. x- and y- of the modified IEEE 123-bus distribution feeder and location of depots.

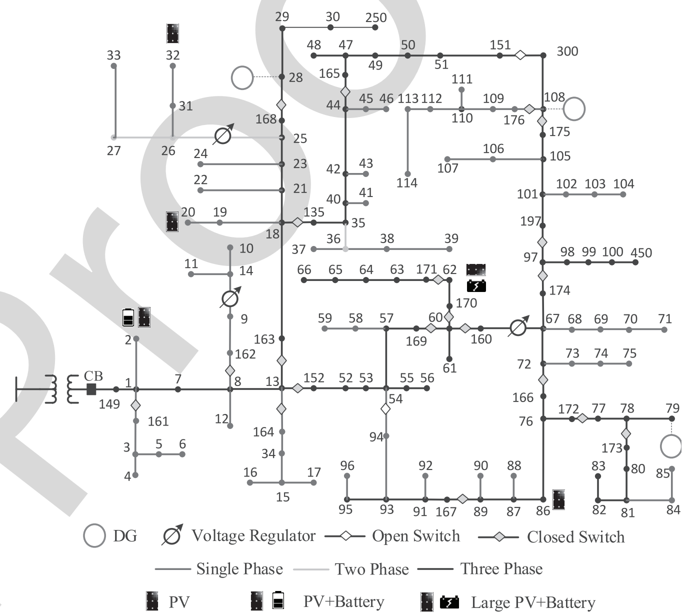

Fig. 7. Modified IEEE 123-bus distribution feeder.

and 500 kW/ 2100 kWh, respectively. Additional details about the network can be found in [33].

We assume that a category 3 hurricane is forecasted to make its way towards the test system. Fig. 8 shows an example of a hurricane landfall and the maximum sustained wind speed. Monte Carlo sampling is used to generate 100 damage scenarios with equal probability. First, lognormal distribution with $\mu = 4.638$ and $\sigma = 0.039$ [24] is used to generate 100 scenarios of possible wind speeds at landfall. Then, the models presented in Section III are used to evaluate the impact of the extreme event. The number of scenarios are reduced to 30 using the tool SCENRED2 in the General Algebraic Modeling System (GAMS) [34] to reduce the computational complexity [35]. The simulation data used in equations (2)–(7) are listed in Table I.

After generating the damage scenarios, the PF problem (12) is solved for each scenario to find the critical lines to be repaired. Then, the SMIP model presented in Section IV is used to model the preallocation problem. It is assumed that there are 5 potential staging areas, the location of each depot

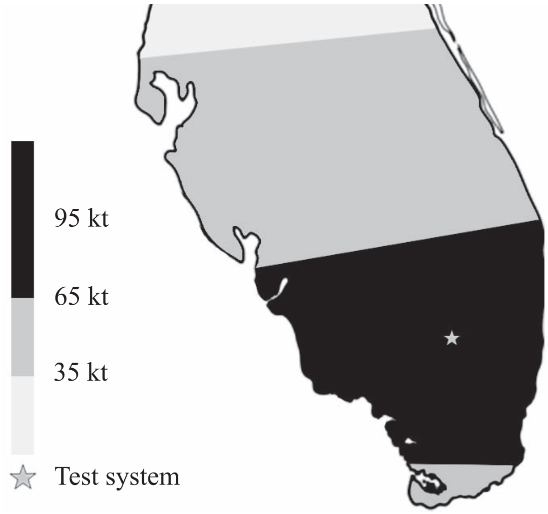

Fig. 8. Maximum wind speed (kt) on test area.

TABLE I
SIMULATION DATA FOR THE FRAGILITY MODELS

Model	Parameter	Value	Ref.
Pole failure	a^p	0.0001	[25]
	b^p	0.0421	
Conductor failure	G_1	1	[27]
	G_2	0.83	
	G_3	1	
	C^f	1.2	
	L_l^c	45.72 m	[36]
	D_l^c	0.0183 m	
	F_l^{force}	62.8 kN	
	$\{a_h, b_h, c_h\}$	$\{$-2.752, 0.680, 0.663$\}$	[28]
	S_l^w	0–1	
	k_l	0.57–1.43	[37]
	$D_H^{b_h}$	0.15 m	[26]

TABLE II
SIMULATION DATA FOR SCRAP ON THE IEEE 123-BUS FEEDER

Parameter	Value
Depot supply capacity (unit)	$\mathcal{C}_d^E$ = {600,400,400,250,250}
Depot crew capacity (crew)	$\mathcal{C}_d^H$ = {8,7,7,5,5}
Capacity required (unit)	$\mathcal{C}_\tau^R$ ={10,8,5,4,6}
Staging areas costs ($)	$\mathcal{P}_d^D$ = {0,170K,170K,90K,90K}
Equipment costs ($/unit*)	$\mathcal{P}_\tau^{EI}$ = {2K,1.2K,2.5K,1.2K,3.3K}
Hourly cost ($/crew)	Line crew: 225, Tree crew: 120
Transportation costs ($/tkm)	0.098
Contracting costs	$4285/crew

*For the conductor, 1km = 1 unit.

is shown in Fig. 6. We set the maximum distance between the staged crews and damaged components to be 16 km ($\bar{D} = 16$ km) in this simulation. Depot 1 is assumed to be the main location of the utility and must be staged ($\nu_1 = 1$). Depot 1 has 5 line crews, 3 tree crews, and a stockpile of 25 poles (10 for 3-phase lines and 15 for 1- and 2-phase lines), 4 km of conductor, 8 single-phase transformers, and 3 three-phase transformers. The utility can obtain additional resources based on the results of the SCRAP model. The data for the costs used in the SCRAP model are presented in Table II [38], [39].

TABLE III
PRE-EVENT PREPARATION RESULTS

		SCRAP		DA		RSO	
Staged Depots		1	4	1	4	1	4
Line Crews		6	4	6	4	6	4
Tree Crews		2	1	2	1	2	1
Equipment	1	10	6	10	0	15	8
	2	16	13	13	6	26	15
	3	3	0	3	0	3	0
	4	6	2	7	1	6	3
	5	3.8 km	2 km	2.5 km	1.5 km	5 km	3 km
Costs		$146,766		$117,443		$183,371	

The penalty costs for the unmet equipment demand is assumed to be 10 times the actual cost of the equipment. As for the penalty cost on the restoration time, we estimate the per hour outage cost $/h. For the IEEE-123 bus system considered in this paper, the average daily load is 2772.75 kW. Using the average per hour cost [41] of $2/kWh for regular loads and $16/kWh for critical loads, the estimated per hour cost is found to be $14610.5/h. We set $\mathcal{P}^R$ to equal half of the estimated per hour cost so that the penalty cost is divided between line repairs and tree removal in (14).

A. Preparation

The SCRAP model is solved using Pyomo with IBM's CPLEX 12.6 mixed-integer solver on a high-performance computing system. The simulation is performed on Iowa State University's Condo cluster, whose individual blades consist of two 2.6 GHz 8-Core Intel E5-2640 v3 processors and 128GB of RAM. Table III presents the results of the preparation problem using SCRAP and PH with 30 scenarios and 1 scenario, which we refer to as deterministic allocation (DA). The single scenario for DA is obtained by reducing the number of scenarios to 1 using SCENRED2. Moreover, the robust stochastic optimization (RSO) method presented in [13] is used to solve the preparation problem. The staging sites and the number of crews are found to be the same for both stochastic and deterministic solutions. However, SCRAP invested around $30,000 more in equipment. The deterministic solution is biased towards a single scenario and did not consider extreme cases where the required number of equipment is high. On the other hand, RSO favors a solution that would perform better with worst-case scenarios. RSO invested around $40,000 more than SCRAP on equipment. However, this can lead to over-preparation and over-investment.

The results of the SCRAP model indicate that Depot 4 should be staged in preparation to the weather event in support to the main location (Depot 1). Five new external line crews are contracted with one positioned at Depot 1 and four positioned at Depot 4. In addition, one tree crew is transferred from Depot 1 to Depot 4. Six 3-phase poles (type 1) are ordered to Depot 4 and fourteen type 2 poles are ordered, one to Depot 1 and thirteen to Depot 4. Also, two single-phase transformers are transferred to Depot 4 from Depot 1. Finally, around 200 meters of conductor is transferred from Depot 1

TABLE IV
PERFORMANCE OF THE STOCHASTIC PROGRAM

Method	Objective Value	Computation Time	EVPI
WS	$513,170	N/A	N/A
SCRAP-EF	$549,554	300 min	$36,384
SCRAP-PH	$551,585	106 min	$38,415
RSO	$608,683	335 min	$95,513
ED	$714,602	2 min	$201,432

to Depot 4, and approximately 1800 meters of conductor is ordered to Depot 4.

To show the importance of considering uncertainty in the problem, we calculate the expected value of perfect information (EVPI)). EVPI is the difference between the wait-and-see (WS) and the stochastic solutions. It represents the value of knowing the future with certainty. WS is the expected value of reacting to random variables with perfect foresight. It is obtained by calculating the means of all deterministic solutions of the scenarios. WS provides a lower bound for the objective value and cannot be obtained in practice. As for evaluating the performance of the deterministic solution across different scenarios, we set the first-stage variables obtained from DA as fixed parameters and solve the stochastic problem. Let $\zeta = \mathrm{F}(\boldsymbol{x}, \boldsymbol{\xi})$ be the stochastic programming problem with first-stage variables $\boldsymbol{x}$ and random variables $\boldsymbol{\xi}$. If x^{DA} is the first-stage solution obtained by solving the deterministic problem, then the expected value of the deterministic solution (ED) is $\zeta^{ED} = \mathrm{F}(\boldsymbol{x}^{\mathrm{DA}}, \boldsymbol{\xi})$. The same approach is used to calculate the objective value of RSO. From Table IV, the stochastic solution from SCRAP with PH is less than ED, which is expected since SCRAP considers the variability of the extreme event outcome unlike the deterministic solution. The difference between PH and ED is $163,017, which is around 80% of the difference between ED and WS. This indicates that the stochastic model leads to a better preparation strategy by acquiring and positioning enough equipment. Solving the two-stage stochastic problem is more beneficial than solving a deterministic problem. PH achieved a solution only 0.36% less than EF with a considerably lower computation time. RSO achieved a solution that outperforms the deterministic one, however, the EVPI for RSO is $95,513 and $38,415 for SCRAP-PH. In addition, RSO requires more computation time when compared to SCRAP-PH.

B. Stability Test

The stability test in [40] is used in this study to check the sensitivity of solution stability to the number of scenarios. The idea of the test is to solve the stochastic problem with multiple independent sets of scenarios and compare the objective values. The model is stable if the objective values are approximately equal [40]. We generate 8 sets of scenarios, each set includes 30 to 100 scenarios. The simulation results are shown in Fig. 9, which shows that the variation of the objective value is small. Therefore, the method is stable and 30 scenarios is adequate for representing the uncertainties.

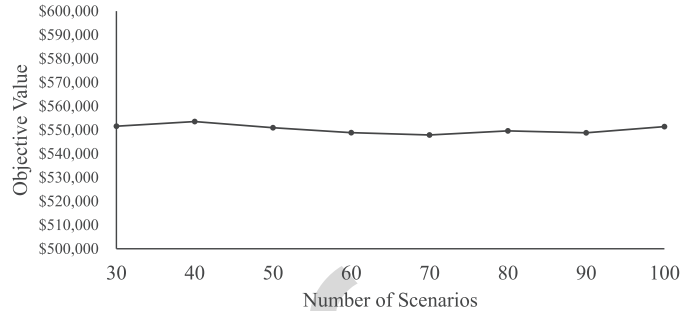

Fig. 9. Sensitivity analysis of optimal objective value versus the number of scenarios.

TABLE V
REPAIR AND RESTORATION PERFORMANCE AFTER THE EVENT

Preparation	Equipment	Load served (kWh)
SCRAP	{+3,+11,+3,+6,+0.32 km}	80,136 kWh
RSO	{+10,+23,+3,+7,+3.7 km}	80,136 kWh
DA	{-3,+1,+3,+6,-0.34 km}	77,448 kWh
W/O Preparation	{-3,-3,+3,+6,-0.34 km}	46,667 kWh

"-": shortage; "+": surplus; the load served is for the first 48 hours
Equipment: {Poles for 3-phase lines, Poles for single-phase lines, 3-phase transformers, single-phase transformers, conductor}

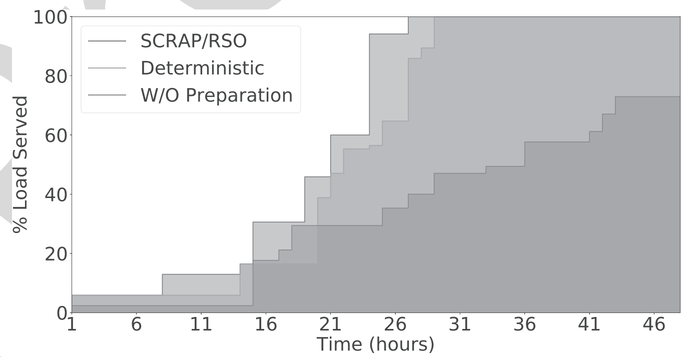

Fig. 10. Post-event percentage of load served.

C. Restoration

After the event impacts the system, it is up to the utility to dispatch the crews and manage the equipment. The efficiency of this process depends on the location of the crews and the amount of stored equipment. To assess the devised preparation plan, we solve the repair and restoration problem [21]. A new random scenario is generated on the IEEE 123-bus system, with crews and equipment allocated according to the results in Table III. In the generated scenario, 13 three-phase poles, 18 single-phase poles, 2 single-phase transformers, and 4343.4 meter of conductor are damaged. The method presented in [21] is used to dispatch the crews and operate the network to restore energy to customers as fast as possible. Four preparation methods are tested: 1- SCRAP; 2- RSO; 3- DA; 4- without preparation (the utility starts with its crews and equipment positioned at Depot 1). The results are shown in Table V and Fig. 10. The "+" sign in Table V indicates a surplus of equipment (number of available equipment is higher than the amount required) and "−" indicates a shortage of equipment. Both SCRAP and RSO over prepare with a large surplus of

11 single-phase poles for SCRAP and 23 single-phase and 10 three-phase poles for RSO. However, the restoration process is faster with 80 MWh served in the first 48 hours for both methods. Without preparation and DA have a shortage of 3 three-phase poles and 0.34 km of conductor. Moreover, without preparation, there is a shortage of 3 single-phase poles. We assume that the equipment required to finish repairs can be obtained 12 hours after the event. With 10 line crews and 3 tree crews, the system can be completely restored within 48 hours (27 and 30 hours with SCRAP/RSO and DA, respectively). On the other hand, it takes more than 48 hours to restore the system for 5 line crews and 3 tree crews. The percentage of load served comparing the three preparation strategies is shown in Fig. 10, where SCRAP has the best performance.

VII. Conclusion

In this paper, a new study for disaster preparation considering crews and equipment allocation is presented. The study starts with analyzing the fragility of distribution networks to extreme events in order to estimate their impacts on the network. Several outcome scenarios are generated providing information on the number of equipment required, estimated repair times, and critical lines. A two-stage stochastic mathematical model is developed to select staging locations, and allocate crews and equipment. A study case is presented on the IEEE 123-bus system where the performance of the proposed model is tested. The results demonstrate the effectiveness of the proposed approach for both meeting the equipment demand and post-event recovery operation. By using an effective preparation procedure, we can ensure that enough equipment is present for repairing the damaged components in the network and facilitate a faster restoration process.

References

[1] M. DeCamp. (Mar. 22, 2018). *Eaton's Blackout Tracker Annual Report Shows 36.7 Million People Affected by More Than 3,500 Power Outages in 2017*. [Online]. Available: http://www.eaton.com/us/en-us/company/news-insights/news-releases/2018/eaton_s-blackout-tracker-annual-report-shows-36-7-million-people.html

[2] S. Ma, S. Li, Z. Wang, and F. Qiu, "Resilience-oriented design of distribution systems," *IEEE Trans. Power Syst.*, vol. 34, no. 4, pp. 2880–2891, Jul. 2019.

[3] G. J. Lim, S. Kim, J. Cho, Y. Gong, and A. Khodaei, "Multi-UAV pre-positioning and routing for power network damage assessment," *IEEE Trans. Smart Grid*, vol. 9, no. 4, pp. 3643–3651, Jul. 2018.

[4] A. Arif, Z. Wang, J. Wang, and C. Chen, "Power distribution system outage management with co-optimization of repairs, reconfiguration, and DG dispatch," *IEEE Trans. Smart Grid*, vol. 9, no. 5, pp. 4109–4118, Sep. 2018.

[5] "Economic benefits of increasing electric grid resilience to weather outages," Executive Office President, Washington, DC, USA, Rep., 2013.

AQ3 [6] *Storm Response and Organized Chaos: Utilities Can Prepare and Plan for the Unpredictable, Utility Products*, PA Consulting Group, London, U.K., Jan. 2013. Accessed: May 14, 2019. [Online]. Available: https://www.utilityproducts.com/home/article/16002960/storm-response-and-organized-chaos-utilities-can-prepare-and-plan-for-the-unpredictable

[7] Z. Li, M. Shahidehpour, F. Aminifar, A. Alabdulwahab, and Y. Al-Turki, "Networked microgrids for enhancing the power system resilience," *Proc. IEEE*, vol. 105, no. 7, pp. 1289–1310, Jul. 2017.

[8] M. Gallucci, *Rebuilding Puerto Rico's Power Grid: The Inside Story*, IEEE Spectr., New York, NY, USA, Mar. 12, 2018. Accessed: May 14, 2019. [Online]. Available: https://spectrum.ieee.org/energy/policy/rebuilding-puerto-ricos-power-grid-the-inside-story

[9] H. O. Mete and Z. B. Zabinsky, "Stochastic optimization of medical supply location and distribution in disaster management," *Int. J. Prod. Econ.*, vol. 126, no. 1, pp. 76–84, 2010.

[10] A. Verma and G. M. Gaukler, "Pre-positioning disaster response facilities at safe locations: An evaluation of deterministic and stochastic modeling approaches," *Comput. Oper. Res.*, vol. 62, pp. 197–209, Oct. 2015.

[11] O. Rodríguez-Espíndola, P. Albores, and C. Brewster, "Disaster preparedness in humanitarian logistics: A collaborative approach for resource management in floods," *Eur. J. Oper. Res.*, vol. 264, no. 3, pp. 978–993, Feb. 2018.

[12] A. Ben-Tal, B. D. Chung, S. R. Mandala, and T. Yao, "Robust optimization for emergency logistics planning: Risk mitigation in humanitarian relief supply chains," *Transport. Res. Part B Methodol.*, vol. 45, no. 8, pp. 1177–1189, Sep. 2011.

[13] A. Bozorgi-Amiri, M. S. Jabalameli, and S. M. J. M. Al-e-Hashem, "A multi-objective robust stochastic programming model for disaster relief logistics under uncertainty," *OR Spectr.*, vol. 35, no. 4, pp. 905–933, Nov. 2013.

[14] M. Fereiduni and K. Shahanaghi, "A robust optimization model for distribution and evacuation in the disaster response phase," *J. Ind. Eng. Int.*, vol. 13, no. 1, pp. 117–141, Mar. 2017.

[15] W. Ni, J. Shu, and M. Song, "Location and emergency inventory pre-positioning for disaster response operations: Min–max robust model and a case study of Yushu Earthquake," *Prod. Oper. Manag.*, vol. 27, no. 1, pp. 160–183, Jan. 2018.

[16] S. Wang, B. R. Sarker, L. Mann, Jr., and E. Triantaphyllou, "Resource planning and a depot location model for electric power restoration," *Eur. J. Oper. Res.*, vol. 155, no. 1, pp. 22–43, May 2004.

[17] P. V. Hentenryck, R. Bent, and C. Coffrin, "Strategic planning for disaster recovery with stochastic last mile distribution," in *Proc. Int. Conf. CPAIOR*, Bologna, Italy, Jun. 2010, pp. 318–333.

[18] C. Coffrin, P. V. Hentenryck, and R. Bent, "Strategic stockpiling of power system supplies for disaster recovery," in *Proc. IEEE Power Eng. Soc. Gen. Meeting*, San Diego, CA, USA, 2011, pp. 1–8.

[19] S. Lei, C. Chen, Y. Li, and Y. Hou, "Resilient disaster recovery logistics of distribution systems: Co-optimize service restoration with repair crew and mobile power source dispatch," *IEEE Trans. Smart Grid*, to be published.

[20] Y. Lin, B. Chen, J. Wang, and Z. Bie, "A combined repair crew dispatch problem for resilient electric and natural gas system considering reconfiguration and DG islanding," *IEEE Trans. Power Syst.*, vol. 34, no. 4, pp. 2755–2767, Jul. 2019.

[21] A. Arif, Z. Wang, J. Wang, and C. Chen, "Repair and resource scheduling in unbalanced distribution systems using neighborhood search," AQ4 *arXiv:1808.10548 [math.OC]*, Aug. 2018.

[22] S. Ma, B. Chen, and Z. Wang, "Resilience enhancement strategy for distribution systems under extreme weather events," *IEEE Trans. Smart Grid*, vol. 32, no. 2, pp. 1440–1450, Mar. 2017.

[23] J. Kaplan and M. De Maria, "A simple empirical model for predicting the decay of tropical cyclone winds after landfall," *J. Appl. Meteorol.*, vol. 34, no. 11, pp. 2499–2512, Nov. 1995.

[24] P. Javanbakht, "Risk-based generation dispatch in the power grid for resilience against extreme weather events," Ph.D. dissertation, Elect. Eng. Comput. Sci. Dept., Colorado School of Mines, Golden, CO, USA, 2015. Accessed: Dec. 12, 2018. [Online]. Available: https://mountainscholar.org/handle/11124/17126

[25] M. Ouyang and L. Dueñas-Osorio, "Multi-dimensional hurricane resilience assessment of electric power systems," *Struct. Safety*, vol. 48, pp. 15–24, May 2014.

[26] J. Winkler, L. Dueñas-Osorio, R. Stein, and D. Subramanian, "Performance assessment of topologically diverse power systems subjected to hurricane events," *Rel. Eng. Syst. Safety*, vol. 95, no. 4, pp. 323–336, Apr. 2010.

[27] C. Bayliss, *Transmission and Distribution Electrical Engineering*. London, U.K.: Butterworth, 1996, pp. 95–106.

[28] C. D. Canham, M. J. Papaik, and E. F. Latty, "Interspecific variation in susceptibility to windthrow as a function of tree size and storm severity for northern temperate tree species," *Can. J. Forest Res.*, vol. 31, no. 1, pp. 1–10, Jan. 2001.

[29] S. D. Ritenour, "Gulf Power Company's vegetation management for storm hardening," Gulf Power Company, Pensacola, FL, USA, Sep. 2006. Accessed: Jan. 12, 2019. [Online]. Available: http://www.psc.state.fl.us/library/filings/2006/08950-2006/

[30] J. R. Birge and F. Louveaux, *Introduction to Stochastic Programming*. New York, NY, USA: Springer, 1997. AQ5

[31] R. T. Rockafellar and R. J.-B. Wets, "Scenarios and policy aggregation in optimization under uncertainty," *Math. Oper. Res.*, vol. 16, no. 1, pp. 119–147, 1991.

[32] W. E. Hart, C. Laird, J. P. Watson, and D. L. Woodruff, *Pyomo—Optimization Modeling in Python* (Springer optimization and Its Applications), vol. 67. New York, NY, USA: Springer, 2012.

AQ6 [33] "123-bus feeder," IEEE PES AMPS DSAS Test Feeder, Working Group, Feb. 2014. Accessed: May 12, 2018. [Online]. Available: http://sites.ieee.org/pes-testfeeders/resources/

AQ7 [34] GAMS/SCENRED2. *Documentation*. [Online]. Available: https://www.gams.com/24.8/docs/tools/scenred2/index.html

[35] A. Golshani, W. Sun, Q. Zhou, Q. P. Zheng, and Y. Hou, "Incorporating wind energy in power system restoration planning," *IEEE Trans. Smart Grid*, vol. 10, no. 1, pp. 16–28, Jan. 2019.

[36] Southwire Company. (Apr. 19, 2012). *Aluminum Conductor. Steel Reinforced*. [Online]. Available: https://www.southwire.com/ProductCatalog/XTEInterfaceServlet?contentKey=prodcatsheet16

[37] L. Kempner, Jr., *Substation Structure Design Guide (ASCE Manuals and Reports on Engineering Practice)*, vol. 113. Reston, VA, USA: ASCE, 2007.

[38] H. R. Lu and A. El Hanandeh, "Environmental and economic assessment of utility poles using life cycle approach," *Clean Techol. Environ. Policy*, vol 19, no. 4, pp. 1047–1066, Oct. 2016.

[39] M. S. Khomami and M. S. Sepasian, "Pre-hurricane optimal placement model of repair teams to improve distribution network resilience," *Elect. Power Syst. Res.*, vol. 165, pp. 1–8, Dec. 2018.

[40] M. Kaut and S. W. Wallace, "Evaluation of scenario-generation methods for stochastic programming," *Stochastic Program.*, vol. 3, no. 2, pp. 257–271, May 2007.

[41] (2018). *Synapse Energy Economics, Avoided Energy Supply Components in New England: 2018 Report*. [Online]. Available: http://www.synapse-energy.com/sites/default/files/AESC-2018-17-080-Oct-ReRelease.pdf

Anmar Arif (S'16) received the B.S. degree in electrical engineering from King Saud University in 2012 and the master's degree from Arizona State University in 2015. He is currently pursuing the Ph.D. degree with the Department of Electrical and Computer Engineering, Iowa State University, Ames, IA, USA. He was a Teaching Assistant with King Saud University and a Research Assistant with Saudi Aramco Chair in Electrical Power, Riyadh, Saudi Arabia, in 2013. His current research interests include power system optimization, outage management, and microgrids.

Zhaoyu Wang (M'15) received the B.S. and M.S. degrees in electrical engineering from Shanghai Jiao Tong University in 2009 and 2012, respectively, and the M.S. and Ph.D. degrees in electrical and computer engineering from the Georgia Institute of Technology in 2012 and 2015, respectively. He is the Harpole-Pentair Assistant Professor with Iowa State University. He was a Research Aid with Argonne National Laboratory in 2013 and an Electrical Engineer Intern with Corning Inc., in 2014. His research interests include power distribution systems, microgrids, renewable integration, power system resilience, and data-driven system modeling. He is the Principal Investigator for a multitude of projects focused on the above areas and funded by the National Science Foundation, the Department of Energy, National Laboratories, PSERC, and Iowa Energy Center. He is the Secretary of IEEE Power and Energy Society Award Subcommittee. He is an Editor of the IEEE TRANSACTIONS ON POWER SYSTEMS, the IEEE TRANSACTIONS ON SMART GRID, and the IEEE POWER ENGINEERING LETTERS, and an Associate Editor of *IET Smart Grid*.

Chen Chen (M'13) received the B.S. and M.S. degrees from Xi'an Jiaotong University, Xi'an, China, in 2006 and 2009, respectively, and the Ph.D. degree in electrical engineering from Lehigh University, Bethlehem, PA, USA, in 2013. From 2013 to 2015, he was a Post-Doctoral Researcher with the Energy Systems Division, Argonne National Laboratory, Argonne, IL, USA, where he is currently an Energy Systems Scientist with the Energy Systems Division. His primary research is in optimization, communications and signal processing for smart electric power systems, power system resilience, and cyber-physical system modeling for smart grids. He is an Editor of the IEEE TRANSACTIONS ON SMART GRID and the IEEE POWER ENGINEERING LETTERS.

Bo Chen (M'17) received the B.S. and M.S. degrees from North China Electric Power University, Baoding, China, and the Ph.D. degree in electrical engineering from Texas A&M University, College Station, TX, USA, in 2017. In 2016, he was a Research Aide with Argonne National Laboratory, Argonne, IL, USA, where he is currently a Post-Doctoral Researcher with the Energy Systems Division. His research interests include modeling, control, and optimization of power systems, cybersecurity, and cyber-physical systems.